

Hybrid Multilevel Thresholding-Otsu and Morphology Operation for Retinal Blood Vessel Segmentation

Erwin, *Member, IAENG*, Arfattustary Noorfizir, Muhammad Naufal Rachmatullah, Saparudin, *Member, IAENG*, Ghazali Sulong

Abstract—This paper proposes an image segmentation method, namely multilevel thresholding-Otsu. The proposed method shows a comparison of different thresholding levels. The thresholding technique used is Otsu. This study uses retinal images from Structured Analysis of the Retina (STARE) dataset. Peak Signal Noise Ratio (PSNR) is a comparison of the values of image quality used to compare the similarities between segmented images and original images. The experimental results show that this method produces high segmentation quality, as seen from the calculation of the average PSNR at the threshold level ($k = 7$) is 39.45 dB, and the average accuracy is 92.53%, Sensitivity is 72.58%, and Specificity is 97.02%.

Index Terms—Blood vessel, multilevel thresholding, Otsu, retina, segmentation

I. INTRODUCTION

BIOMETRICS is a technology that uses biological characteristics to identify individuals[1]. Some biological characteristics for identification purposes include retina[2],[3], face[4],[5],[6], and iris[7]. The retina has a spherical surface[2]. The retina is useful for coating the inner surface of the eye which contains light-sensitive cells (photoreceptors). Retinal images provide information in the form of vascular retinal structures that are common in retinal diseases. These diseases usually change the pattern of blood vessel[8]. The retina has a unique vein pattern [1], smooth and small. Unfortunately, the introduction of the theory of the retina is quite complicated. One of the first steps after initial processing is segmentation.

Image segmentation is a fundamental technique in image processing and computer vision that helps medical experts diagnose an illness [2][9]. Segmentation is the process of repairing, modifying, and simplifying images to be easily

used to analyze diseases. In the analysis of retinal images, retinal vessel segmentation is a topic that has been widely developed and is widely found in the literature[10]. Accurate segmentation of retinal vessels has become a prerequisite for the diagnosis system. The segmentation process is quite complicated, and there are several steps taken in the segmentation process. One of the most important segmentation approaches is thresholding. Thresholding is a simple and effective method of separating objects and backgrounds. Bilevel is an image that has been segmented into two classes, and for segmenting many classes is called Multilevel Thresholding[11]. Otsu is a method commonly used in Multilevel Thresholding (Multithresh). In [11], Otsu combined with the Improved Harmony Search Algorithm (IHSA) method was used to find vector solutions by increasing accuracy, but the experiments carried out were not specific to the retina, even for tongue segmentation better than the retina. In Multithresh, there are a number of methods that have been successfully implemented, some of which are Improved Firefly Algorithm (IFA), which is used to reduce the spots on images that require a long time, which is examined by Kai Chen et al[12]. Particle Swarm Optimization (PSO) which shows that the algorithm has been studied by Yi Liu et al[13] shows the Global Particle Swarm Optimization (GPSO) convergence time needed. The experiment with the Convergent Heterogeneous Particle Swarm Optimization (CHPSO) method carried out by Mohammad Hamed et al[14] have a fairly low standard deviation. Experiments carried out by Habba Maryam et al[15].

In this research, the proposed segmentation technique is the Otsu Multilevel Thresholding-Combined with morphological operations. This method will produce a segmentation of the images presented in the results of morphological operations. In order to shorten the proposed method, it is named Multithresh-Otsu with Morphology Operation (MTO-M). The technique used is expected to help to improve the quality of segmentation. Increasing the quality of this segmentation will be measured using the Peak Signal to Noise Ratio (PSNR) calculation. This paper will be presented in several sections. In the second part, Multilevel Thresholding with Otsu (MTO) will be introduced. The third part will present the experiment and the experimental results that will be discussed by calculating the PSNR and Accuracy. In order to refine the Segmentation results, morphological operations are conducted. The morphological operation can separate blood vessels from the

Manuscript received May 23, 2019; revised November 27, 2019.

Erwin, Arfattustary Noorfizir are with the Department of Computer Engineering, Faculty of Computer Science, Sriwijaya University, Indralaya Ogan Ilir 30662, Indonesia (e-mail: erwin@unsri.ac.id; tnoorfizir@gmail.com).

Saparudin, and Muhammad Naufal Rachmatullah are with the Department of Informatic Engineering, Faculty of Computer Science, Sriwijaya University, Indralaya - Ogan Ilir 30662, Indonesia (e-mail: saparudinmasyarif@gmail.com; naufalrachmatullah@gmail.com).

Ghazali Sulong is with the Centre For Cyber Security & Big Data, Management & Science University, Selangor, Malaysia (e-mail: ghazali_sulong@msu.edu.my).

background based on their shape. The last section concludes from all the experiments conducted.

II. MULTILEVEL THRESHOLDING WITH OTSU METHOD

Segmentation is a process that converts original images into constituents or regional objects. Segmentation aims to separate each component from the image. The quality of the segmentation process will be measured from the obtained accuracy. The better the object is recognized, the higher the accuracy obtained. Image thresholding is an image processing technique that divides or separate one image into several objects to detect various areas based on the same colour or grey level intensity. One of the most important things in the segmentation process is to find a threshold value [16]. In multilevel thresholding, the main task is to choose the appropriate threshold value using an iterative process.

The threshold is the process in which the pixels of a grayscale image is divided into several classes depending on the level of intensity (L). In this research threshold value (TH) calculated using (1):

$$\begin{aligned} Cl_1 &\leftarrow q \text{ if } 0 \leq q < TH, \\ Cl_2 &\leftarrow q \text{ if } TH \leq q < L - 1, \end{aligned} \quad (1)$$

where q is one of $m \times n$ pixels of the grayscale image that can be represented in L grayscale levels $L = \{0, 1, 2, \dots, L - 1\}$. Cl_1 and Cl_2 are the classes where pixel q can be found, while TH is the threshold. The rules in (1) correspond to the bi-level threshold and can be easily extended to several sets:

$$\begin{aligned} Cl_1 &\leftarrow q \text{ if } 0 \leq q < TH_1, \\ Cl_2 &\leftarrow q \text{ if } TH_1 \leq q < TH_2, \\ Cl_n &\leftarrow q \text{ if } TH_n \leq q < TH_{n+1}, \\ Cl_m &\leftarrow q \text{ if } TH_m \leq q < L - 1, \end{aligned} \quad (2)$$

where $\{TH_1, TH_2, \dots, TH_n, TH_{n+1}, TH_k\}$ represent different thresholds. The problem for bilevel and multilevel thresholding is to choose the TH value that identifies the class correctly. Although the Otsu are well-known approaches for determining these values, Otsu propose different objective functions that must be maximized to find the optimal threshold value, as discussed below.

Otsu uses maximum variance values from different classes as criteria for image segmentation. Taking the level of intensity L from a grayscale image or from each component of an RGB image (red, green, and blue), the probability distribution of intensity values is calculated as follows[17]:

$$\begin{aligned} Pp_a^c &= \frac{p_a^c}{P_{tot}^c}, \quad p_a^c \geq 0, \quad \sum_{a=1}^{P_{tot}^c} Pp_a^c = 1, \\ c &= \begin{cases} 1, 2, 3, & \text{if RGB Image,} \\ 1, & \text{if Grayscale Image,} \end{cases} \end{aligned} \quad (3)$$

Where :

- a = gray level intensity (L) ($0 \leq a \leq L-1$)
- c = component, the value specified from i or RGB
- p_{tot} = the total pixel of the image
- p_a^c = histogram (the number of pixels corresponds to the intensity in c)
- Pp_a^c = probability of distribution

For bilevel two classes segmentation the formula defined as follow:

$$\begin{aligned} Cl_1 &= \frac{Pp_a^c}{W_0^c(TH)}, \dots, \frac{Pp_{TH}^c}{W_0^c(TH)}, \\ Cl_2 &= \frac{Pp_{TH+1}^c}{W_1^c(TH)}, \dots, \frac{Pp_L^c}{W_1^c(TH)}, \end{aligned} \quad (4)$$

where $W_0^c(TH)$ and $W_1^c(TH)$ are probability distributions for Cl_1 and Cl_2 , as indicated by

$$W_0^c(TH) = \sum_{a=1}^{TH} Pp_a^c, \quad W_1^c(TH) = \sum_{a=TH+1}^L Pp_a^c. \quad (5)$$

It is necessary to calculate the average level μ_0^c and μ_1^c which defines the class using (6). After the values are calculated, the variance between classes σ^{2c} is calculated using (7) defined as follows:

$$\mu_0^c = \sum_{a=1}^{TH} \frac{aPp_a^c}{W_0^c(TH)}, \quad \mu_1^c = \sum_{a=TH+1}^L \frac{aPp_a^c}{W_1^c(TH)}, \quad (6)$$

$$\sigma^{2c} = \sigma_1^c + \sigma_2^c. \quad (7)$$

Note that for both equations, (6) and (7), c depends on the type of image. In (7) number two is part of the Otsu variant operator and does not represent exponents in the mathematical sense. Besides that σ_1^c and σ_2^c in (7) are variants of Cl_1 and Cl_2 which are defined as

$$\sigma_1^c = W_0^c(\mu_0^c + \mu_T^c)^2, \quad \sigma_2^c = W_2^c(\mu_1^c + \mu_T^c)^2, \quad (8)$$

where $\mu_T^c = W_0^c \mu_0^c + W_1^c \mu_1^c$ and $W_0^c + W_1^c = 1$. Based on the values σ_1^c and σ_2^c , (13) presents the objective function:

$$J(TH) = \max(\sigma^{2c}(TH)), \quad 0 \leq TH \leq L - 1, \quad (9)$$

Where $\sigma^{2c}(TH)$ is the Otsu variant for the given th value. Therefore, optimization problems are reduced to find the intensity level (TH) that maximizes (9).

The Otsu method is applied to one image component. In the case of RGB images, it is necessary to apply separation to a single component image. The previous description of

the bilevel method can be expanded to identify multiple thresholds. Considering the k threshold, it is possible to separate the original image into k classes using (2); it is necessary to calculate the variance k and the respective elements. The objective function $J(TH)$ in (9) can thus be rewritten for some thresholds as follows:

$$J(TH) = \max(\sigma^{2^c}(TH)),$$

$$0 \leq TH_a \leq L - 1, a = 1, 2, \dots, k. \quad (10)$$

where $\mathbf{TH} = [TH_1, TH_2, \dots, TH_{k-1}]$, is a vector that contains several thresholds and the variance is calculated through

$$\sigma^{2^c} = \sum_{a=1}^k \sigma_a^c = \sum_{a=1}^k W_a^c (\mu_a^c - \mu_T^c)^2. \quad (11)$$

Here, a represents a class, W_a^c and μ_a^c , respectively, probability of occurrence and class. In multilevel thresholding, these values are obtained as

$$W_0^c(TH) = \sum_{a=1}^{TH_1} Ph_a^c,$$

$$W_1^c(TH) = \sum_{a=TH_1+1}^{TH_2} Ph_a^c,$$

$$\vdots$$

$$W_{k-1}^c(TH) = \sum_{a=TH_{k-1}+1}^L Ph_a^c, \quad (12)$$

And, for average values

$$\mu_0^c = \sum_{a=1}^{TH_1} \frac{aPh_a^c}{W_0^c(TH_1)},$$

$$\mu_1^c = \sum_{a=TH_1+1}^{TH_2} \frac{aPh_a^c}{W_0^c(TH_2)},$$

$$\vdots$$

$$\mu_{k-1}^c = \sum_{a=TH_{k-1}+1}^L \frac{aPh_a^c}{W_1^c(TH_k)}. \quad (13)$$

Similar to the bilevel case, for the multilevel thresholding using the Otsu's method, c corresponds to the image components, RGB $c = 1, 2, 3$, and gray scale $c = 1$.

Steps in the Otsu thresholding process can be seen in the Figure 1.

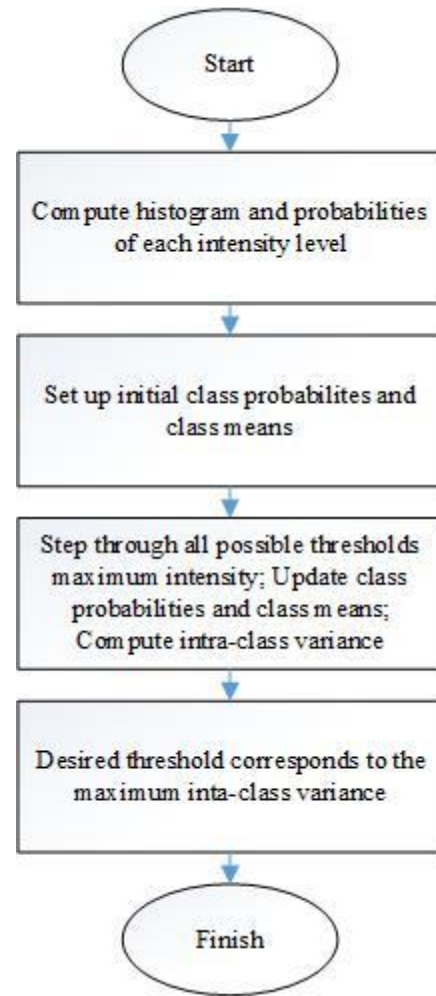


Fig 1. Process Diagram Multilevel Thresholding Otsu

III. RESULT AND ANALYSIS

This experiment was implemented in MATLAB R2018a on Intel® Core™ i5, 2.30Gz, 4.00GB RAM personal computers with the Windows 10 Professional system. In order to validate our proposed method, we use the STARE (Structured Analysis of the Retina) dataset, which consist of 400 retinal images. In this experiment only forty images were tested based on the ground truth dataset. Twenty images are hand-labelled by Adam Hoover (Expert 1), and the others are by Valentina Kouznetsova(Expert 2)[18].

In this study, the original image from the dataset is an RGB image, an RGB image consisting of 3 channels (red, green, and blue). In the blue channel marked by low contrast can be seen in Table I. On the other hand, the red channel is close to the vessels colour. Unfortunately, in the final results for some images there are vessels that are not segmented properly. In order to compare the final result of blood vessels segmentation in the retina image, the histogram of red, green, and blue channels are presented as can be seen in Table I.

TABLE I
COMPARISON OF RED, GREEN AND BLUE CHANNEL RESULTS

	Image				
	im0005	im0081	im0239	im255	im291
Image					
Histogram					
Red Channel					
Green Channel					
Blue Channel					

The resolution of testing data is 700 x 605 in RGB colour space. The images are converted into grey-level image. In this experiment we use the green canal as the grayscaleing method and the result shown in Figure 2 (a). The process of taking this green channel is critical for the next process. Furthermore, contrast enhancement using Contrast Limited Adaptive Histogram Equalization (CLAHE) is performed. After the retinal image through image enhancement step, the

blood vessels are more prominent. The result of this process is shown in Figure 2 (b). Before continued to the thresholding process, the images are filtered first using Multidimensional Filtering (average filter) seen in Figure 2 (c). After filtering process, the multi-level thresholding is performed. The result images are binarized using Otsu multilevel thresholding with seven-level iteratively, as shown in Figure 2 (d).

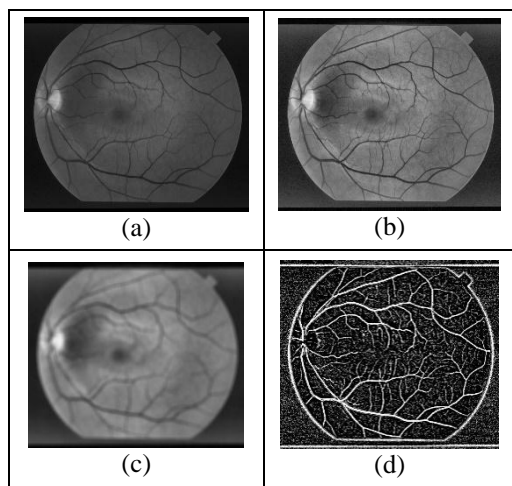


Fig.2. Images im0255. (a) Green Channel, (b) CLAHE, (c) Multidimensional Filtering and (d) Multilevel Thresholding-Otsu

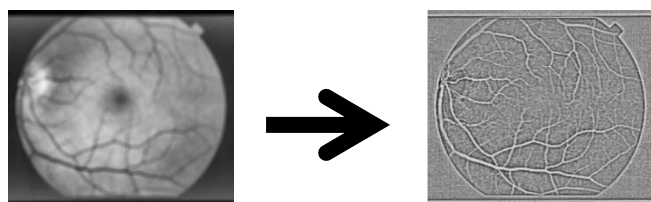


Fig.3. The results of the Otsu Multilevel Thresholding process on im0081

Multilevel is a thresholding technique that aims to choose the appropriate threshold value. This process takes input from multidimensional filtering process. The results of the reduction will be thresholded using a threshold value from level 7. The results of this process can be seen in Figure 3. Level 7 is the best. Comparison of the results of the threshold value can be seen in Table II.

In the Multilevel thresholding process, we implemented thresholding for 5 different levels, namely, 5, 6, 7, 8, and 9. Each level showed significantly different results if it had been carried out until the morphological process.

After the thresholding process, the next step is to remove the noise that is not permeable to the blood vessel. The type of noise occurred is salt-and-paper noise. This removal process can be done on binary images. The results of the process of removing small objects can be seen in Figure 4

The final step is the application of morphology closing in the binarized images. Morphological operation is the post-processing method based on the shape and pattern of images. Mathematical morphology is a non-linear filter method that can be used for image processing, including noise removal, feature removal, edge detection, image segmentation, shape recognition, texture analysis, restoration, reconstruction, compression, and more. Basic mathematical morphological operations will change the composition of the components in the picture and execute fundamental activities on junctions and unions at the same moment. The results of the morphological operation process can be seen in Figure 5. Morphological-based processing can be considered as a bridge between signal and

TABLE II

COMPARISON OF THE RESULTS OF THE THRESHOLD VALUE IM0081

Th	Multilevel Thresholding Otsu	Segmentation Results
5		
6		
7		
8		
9		

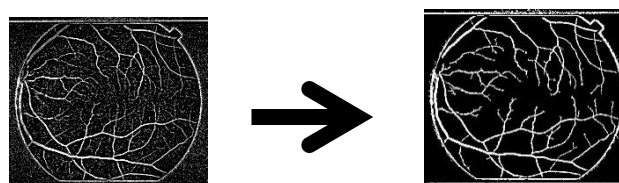


Fig.4. The process of removing small pixels on im0081

image pattern properties. In the morphological operation, there are several processes applied including dilation, erosion, opening and closing. Closing is a process of refining the contour section by combining a narrow gap and a long thin gap and removing small holes in the contour. Can be seen in figure 6.(a) The closing morphological equation can be defined as

$$I \cdot J = (I \oplus J) \ominus J. \tag{14}$$

The above equation can be interpreted as dilation I by J, followed by the erosion of the results by J. I is the original image and J is Structuring Element (SE). Where dilation is a widening operation that works based on convolution, the size of the image is expanded and becomes larger than the SE and the original object. The dilation process focuses on correcting damaged characters, and as a side effect, the character width becomes thicker, which can be seen in figure 6.(b). While erosion is a process that has output as vertical and horizontal lines. The lines basically narrow the width of the image character. Can be seen in figure 6.(c)[19]

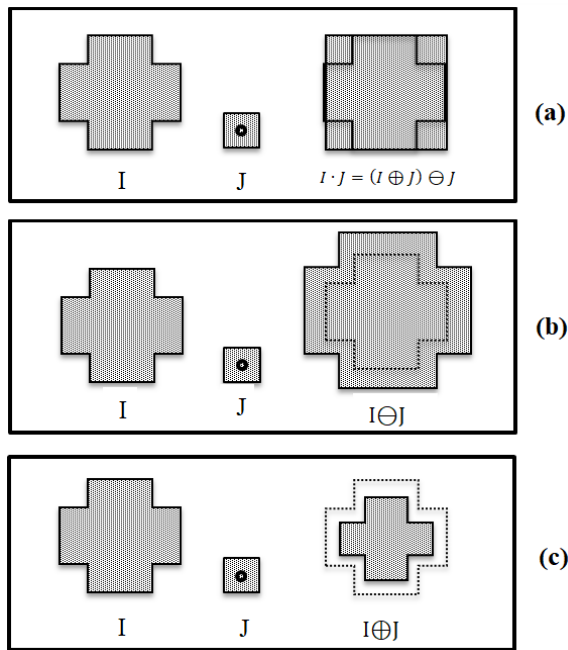


Fig.6. Morphology Operation : (a). Morphology Closing, (b). Dilation, (c) Erosion

After performing morphological operations, to complete the image, the process of refining the circle at the ends of blood vessels is carried out by making a retina mask. The pixel value of the results of making the retina mask will be used as a subtraction value against the pixel values that exist in the results of the morphological operation process.

In the process of making a retina mask, the first step is to change the original image into grayscale, regardless of the 3 colour channels. This change is intended so that the next process can be done. The next process can only accept input in the form of 2-dimensional images. After the image becomes grayscale next is to apply the operation to select the desired area, this operation is commonly called the Region of Interest (ROI). The results of ROI operations can be seen in Figure 7.

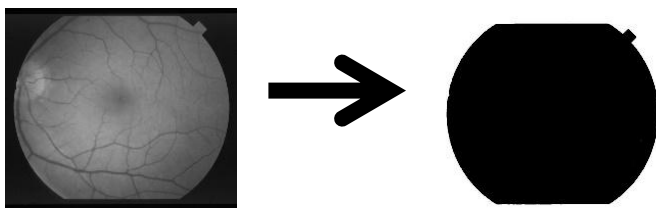


Fig.7. The results of the *region of interest* process on im0081

After the mask-making process, the final step to get the perfect result is to subtract the results of the morphological operation to be subtracted from the mask that was made. The reduction meant is the reduction between pixels, as presented in Figure 8. The results of the blood vessel segmentation can be seen in figure 9. All steps showed in the flow chart diagram presented in Figure 12.

605x700 logical						
	1	2	3	4	5	6
1	0	0	0	0	0	0
2	0	0	0	0	0	0
3	0	0	0	0	0	0
4	0	0	0	0	0	0
5	0	0	0	0	0	0
6	0	0	0	0	0	0
7	0	0	0	0	0	0
8	0	0	0	0	0	0
9	0	0	0	0	0	0
10	0	0	0	0	0	0
11	0	0	0	0	0	0
12	0	0	1	1	0	0

(a)

605x700 logical						
	1	2	3	4	5	6
1	1	1	1	1	1	1
2	1	1	1	1	1	1
3	1	1	1	1	1	1
4	1	1	1	1	1	1
5	1	1	1	1	1	1
6	1	1	1	1	1	1
7	1	1	1	1	1	1
8	1	1	1	1	1	1
9	1	1	1	1	1	1
10	1	1	1	1	1	1
11	1	1	1	1	1	1
12	1	1	1	1	1	1

(b)

605x700 double						
	1	2	3	4	5	6
1	-1	-1	-1	-1	-1	-1
2	-1	-1	-1	-1	-1	-1
3	-1	-1	-1	-1	-1	-1
4	-1	-1	-1	-1	-1	-1
5	-1	-1	-1	-1	-1	-1
6	-1	-1	-1	-1	-1	-1
7	-1	-1	-1	-1	-1	-1
8	-1	-1	-1	-1	-1	-1
9	-1	-1	-1	-1	-1	-1
10	-1	-1	-1	-1	-1	-1
11	-1	-1	-1	-1	-1	-1

(c)

Fig.8. The reduction process in im0081: (a) The results of the morphological operation process, (b) The results of the ROI process, and (c) The final results of the reduction process.

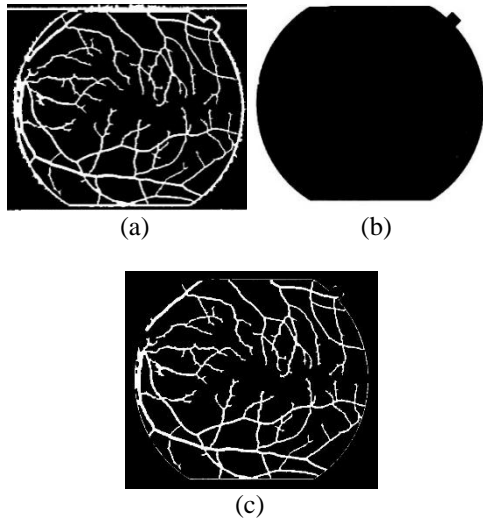


Fig.9. The final segmentation process at im0081: (a) The results of the morphological operation process, (b) The results of the ROI process, and (c) The final results of the segmentation process

Peak Signal to Noise Ratio (PSNR) is one of the parameters for image segmentation validation and its function as the image quality determinant after the image processing process. PSNR is a comparison of values that determine the quality of the image. To find the value of PSNR, we calculate the Mean Square Error (MSE). MSE is the average error value of the difference in the value of processed images and unprocessed images[20]. The PSNR value can determine how well the image segmentation has been done. The unit of PSNR value is expressed in decibel (dB). The PSNR value can be categorized as good if PSNR ≥ 30 dB[11]. The results of the PSNR calculation are shown in Table III. Decreasing the value of PSNR to the threshold value can be seen in Figure 10. After obtaining the best level through calculations, then doing the $k = 7$ segmentation process using morphological operations images can be seen in Table IV.

The PSNR value is shown in equation (15) and the root of the MSE value is shown in equation (16):

$$PSNR = 20 \log_{10} \left(\frac{255}{RMSE} \right) \quad (15)$$

$$RMSE = \sqrt{\frac{1}{row \times column} \sum_{i=1}^{row} \sum_{j=1}^{column} [I(i,j) - \hat{I}(i,j)]^2} \quad (16)$$

where :

I = Image before segmentation

\hat{I} = Image after segmentation

$row \times column$ = The sum of the rows and columns of the image

In order to assess the performance of the segmentation results, this case used to measure data compatibility with the dataset is the Confusion Matrix based on binary images. Confusion Matrix is a parameter method used to measure the compatibility of data with a binary-based dataset. Accuracy, Sensitivity, Specificity and F1 Score were calculated. The value of each performance is obtained from

Equations (17), (18), (19) and (21):

$$Accuracy = \frac{TP + TN}{TP + TN + FN + FP} \quad (17)$$

$$Sensitivity = \frac{TP}{TP + FN} \quad (18)$$

$$Specificity = \frac{TN}{TN + FP} \quad (19)$$

$$Precision = \frac{TP}{TP + FP} \quad (20)$$

$$F1 \text{ Score} = 2 \frac{\frac{TP}{TP + FP} * \frac{TP}{TP + FN}}{\frac{TP}{TP + FP} + \frac{TP}{TP + FN}} \quad (21)$$

True Positive is the number of images that have been properly segmented. Consider the prediction problem of two classes (binary classification), in this experiment the first class is well segmented (g) and the second class is not well segmented (b). The purpose of the calculation is to evaluate the similarity between segmented images and ground truth images hand-labelled by Adam Hoover(Expert 1) and Valentina Kauznetsova (Expert 2). Performance calculations can be seen in Table V.

To compare the performance of the proposed method and from the existing methods, it is presented in Table VI.

There are four possible results from binary classification.

1. True Positive(TP) is if the result of a prediction is g and the actual value is also g.
2. False Positive (FP) is if the result of a prediction is g and the actual value is b.
3. True Negative(TN) is if the result of the prediction is b and the true value is also b.
4. False Negative(FN) is if the result of a prediction is b and the actual value is g.

Based on the formula of the various parameters, the value of Accuracy, Sensitivity, and Specification of True Negative (TN), False Positive (FP), False Negative (FN), and True Positive (TP) each has provisions. Accuracy value is a value that illustrates how strong the results of the match and the system can be matched based on the dataset correctly means that the compatibility in terms of pixels has similarities starting from the shape, size, location, etc. are the same as the dataset concerned. Whereas the Sensitivity value can be defined as the ratio of properly classified retinal artery pixels to the number of retinal artery pixels in ground truth, and the Specification value describes the number of positive category data that are matched based on a dataset correctly divided by the total data that is matched based on a positive dataset meaning how the value of the segmentation process is deeper and more detailed without changing the pixels on its part. Whereas Precision is the number of positive samples classified correctly as a category divided by the total samples classified as positive samples and F1 Score is a comparison of weighted average precision and recall.

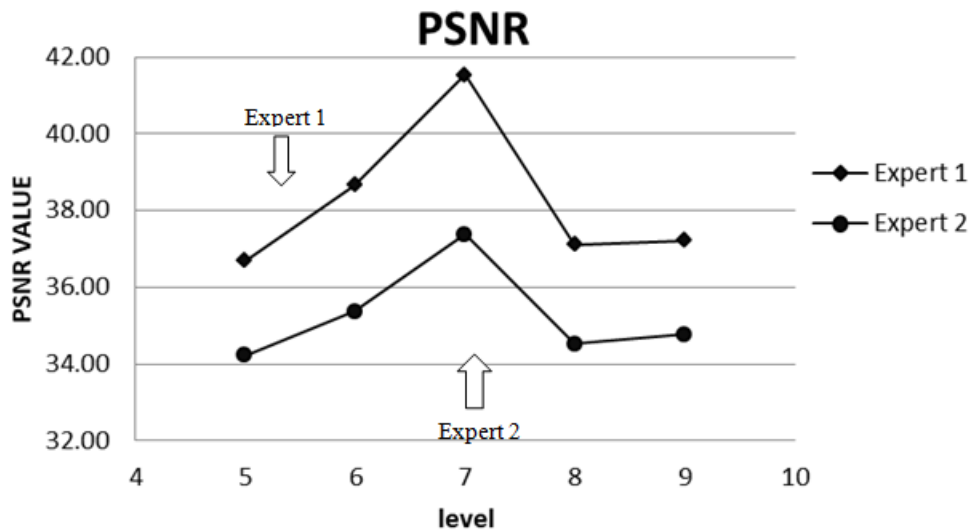


Fig 10. Diagram of PSNR value against several threshold level

TABLE III

CALCULATION OF PSNR MULTILEVEL THRESHOLDING-OTSU AND MORPHOLOGY USING ORIGINAL IMAGES BY ADAM HOOVER AND VALENTINA KOUZNETSOVA

Images	k	PSNR(dB)	
		Adam Hoover [13]	Valentina Kouznetsova [13]
		Expert 1	Expert 2
im0077	5	37.4299	34.4822
	6	38.5158	34.9625
	7	42.5387	37.6877
	8	36.3245	33.7828
	9	36.6078	34.1428
im0081	5	36.2660	33.2988
	6	38.0959	34.0977
	7	41.6865	36.0221
	8	36.2500	33.2385
	9	36.3897	33.3502
im0163	5	37.6644	35.1585
	6	40.8565	37.0689
	7	42.6419	38.7680
	8	39.0571	36.0000
	9	39.5498	36.5829
im0236	5	36.4186	34.2028
	6	39.1053	35.8953
	7	41.0774	37.3896
	8	37.8832	35.1988
	9	35.4200	33.6514
im0239	5	35.7047	33.7974
	6	36.6121	34.4047
	7	40.4154	37.1704
	8	35.2842	33.5226
	9	36.7790	34.8097
im0255	5	36.6020	34.4330
	6	38.7644	35.7686
	7	40.8044	37.1845
	8	37.8523	35.3544
	9	38.6028	36.0756

F1 Score is the average of precision (20) and sensitivity (18) [21], which is used to compare the ground truth and segmentation results. Diagram for F1 Score can be seen in Figure 11. The Diagram presents the results of data on the 20 Retina STARE images. The measurement parameters shown are the F1 score with varying values ranging from 42% to 74%. The diagram shows that the best calculation of F1 score is in the image im0324 (expert 1 or Adam Hoover’s Ground Truth) which is equal to 73.51% (expert 1 or Adam Hoover’s Ground Truth) and im0001 (expert 2 or Valentina Kouznetsova’s Ground Truth) with the value of 66.97%. The lowest F1 score is owned by image im0162 (expert 1 and expert 2) with a value of 51.33% and 42.70%.

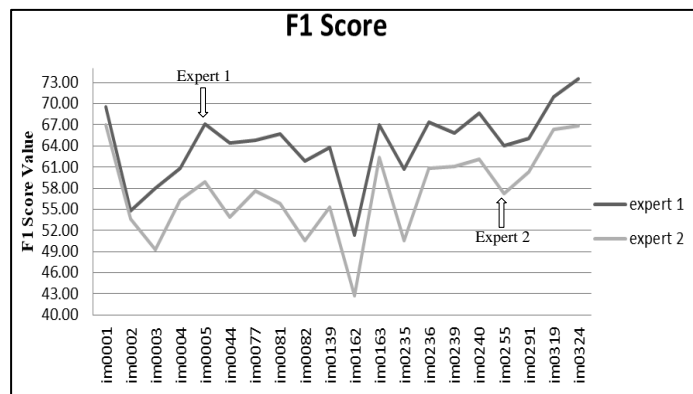


Fig 11. Diagram of F1 Score

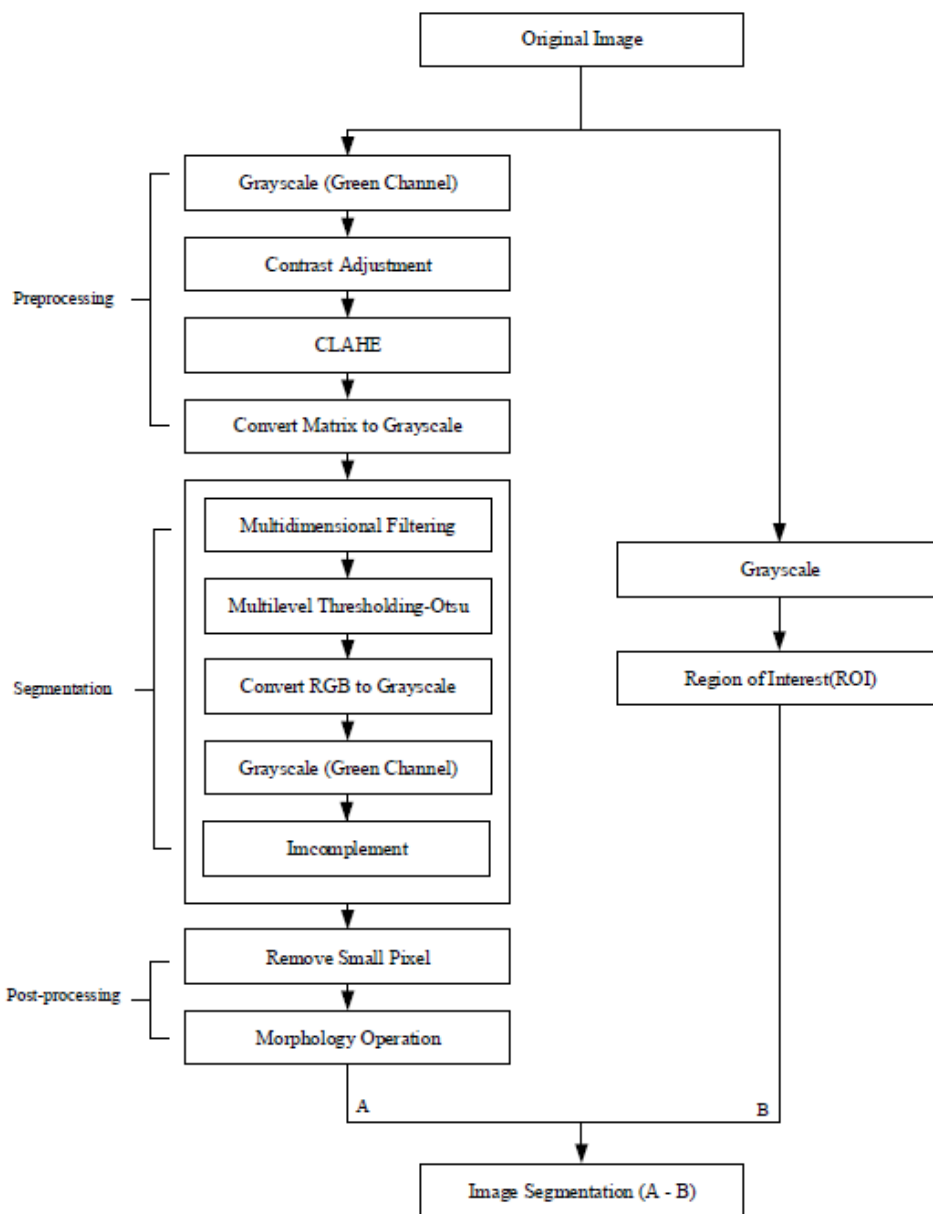


Fig 12. Image Segmentation Process Diagram

TABLE IV

RESULT OF IMAGES SEGMENTATION OF THE OTSU LEVEL THRESHOLDING PROCESS WITH MORPHOLOGY K=7

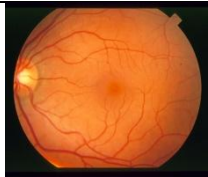
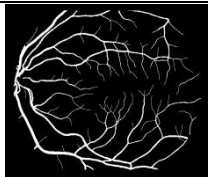
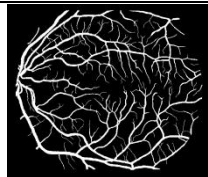
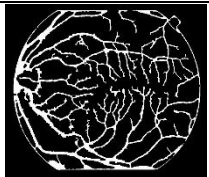

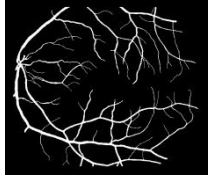
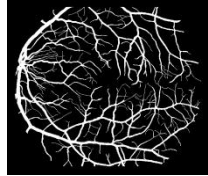
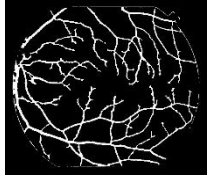
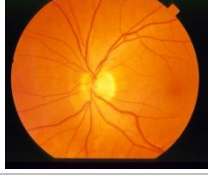
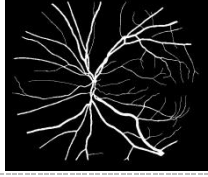
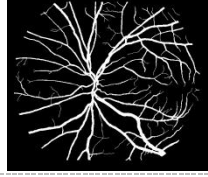
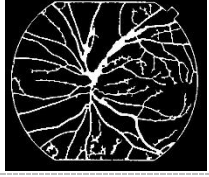

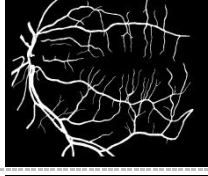
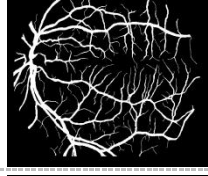


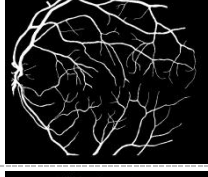
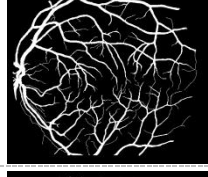
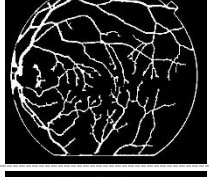
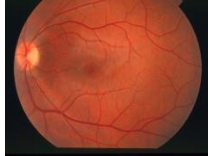
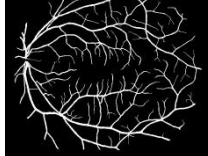
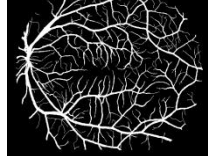

File Images	Original Images	Ground Truth-Segmentation		Proposed Method
		Expert 1	Expert 2	
im0077				
im0081				
im0163				
im0236				
im0239				
im0255				

TABLE V

CALCULATION OF ACCURACY, SENSITIVITY, SPECIFICITY BASED ON GROUND TRUTH STARE

Image	The proposed method with expert 1				The proposed method with expert 2			
	Acc (%)	Sn (%)	Sp (%)	F1 Score (%)	Acc (%)	Sn (%)	Sp (%)	F1 Score (%)
im0001	92.46	71.84	95.26	69.53	91.62	71.81	94.28	66.97
im0002	95.13	75.53	95.93	54.79	94.89	75.60	95.67	53.61
im0003	95.45	73.34	48.01	58.03	93.50	72.59	94.45	49.29
im0004	95.36	72.15	96.58	60.78	94.35	72.56	95.50	56.37
im0005	93.37	71.47	95.66	67.12	90.70	71.39	92.69	58.92
im0044	93.85	70.43	95.86	64.48	90.96	70.78	92.59	53.84
im0077	92.39	71.01	94.74	64.84	90.20	71.35	92.14	57.66
im0081	93.22	73.80	95.09	65.73	90.45	74.62	91.84	55.76
im0082	92.97	72.36	94.74	61.89	89.59	72.44	90.95	50.55
im0139	92.43	70.62	94.70	63.81	90.31	71.15	92.07	55.26
im0162	92.43	73.36	93.53	51.33	89.96	74.44	90.78	42.70
im0163	92.98	72.97	95.88	66.97	91.66	73.57	93.54	62.43

im0235	93.53	71.01	95.24	60.76	91.30	71.23	92.64	50.59
im0236	93.19	74.07	95.20	67.43	91.37	74.13	93.08	60.81
im0239	92.78	74.89	94.61	65.84	91.64	75.10	93.23	61.08
im0240	92.40	71.11	95.23	68.72	90.27	71.42	92.64	62.11
im0255	91.18	72.11	93.52	64.08	88.85	72.38	90.74	57.18
im0291	95.80	74.51	96.98	65.09	94.97	75.17	96.03	60.29
im0319	94.74	70.58	97.16	71.01	93.53	70.83	95.78	66.31
im0324	93.75	71.64	96.80	73.51	91.60	71.76	94.26	66.86
Average	93.47	72.44	93.04	64.29	91.59	72.72	93.18	57.43

TABLE VI

COMPARISON OF THE PERFORMANCE OF THE PROPOSED METHOD AND FROM THE EXISTING METHOD

Method	Performa		
	Accuracy (%)	Sensitivity (%)	Specificity (%)
A. Maharjan <i>et al</i> [8]	95.08	67.74	97.51
L. Câmara Neto <i>et al</i> [22]	88.94	83.44	94.43
Proposed Method	92.53	72.58	97.02

IV. ANALYSIS AND EVALUATION

Table I presents a partial calculation of the PSNR value for segmented images using the proposed method, namely multilevel thresholding-Otsu and morphological operations. The PSNR value is calculated by comparing the results of segmentation with the original image. The original image used is a ground-truth label image from Adam Hoover (Expert 1) and Valentina Kauznetsova (Expert 2) [13]. Tests for all images from the Stare dataset showed that the results of segmentation were very good with a value of > 35 dB for Adam Hoover and Valentina Kauznetsova. These results indicate that the proposed method can segment very well and robustly with $k = 7$. When compared to the results of segmentation for the proposed method with both ground-truth datasets, the result of segmentation for Adam However is better than Valentina Kauznetsova. The results of vascular segmentation in Table II show an improvement in the quality of the segmented blood vessels to be clearer than those of the blood vessels of Adam Hoover and Valentina Kauznetsova. Thin blood vessels look clearer, and more are successfully segmented. Performance measurement for the value of accuracy, sensitivity and specificity in Table VI produces an average value of 91.73%, 47.48%, and 98.29% respectively for the proposed method against Adam Hoover, while for Valentina Kauznetsova the values are 88.59%, 47.37%, respectively and 95.75%. Table IV presents a comparison of the performance of the proposed method with the results obtained by A. Maharjan *et al* [8] and L. Câmara Neto *et al* [22]. When compared with the method used by A. Maharjan *et al* [8] there was a significant value of accuracy, sensitivity and specificity decreased by 5%, 20% and <1%. While the results of the accuracy and sensitivity of the proposed method compared with L. Câmara Neto *et al* [22], there were improvements in the value of 2% and the values of sensitivity and specificity decreased by 36% and <1%.

V. CONCLUSION

In this paper, the method presented is Multilevel Thresholding with Otsu. Calculation of Peak Signal to Noise Ratio (PSNR) is done to see whether the segmentation has

been done well.

This calculation assesses the quality of segmentation by considering the image before segmentation and image after segmentation. The results of the experiments conducted showed that the exposure of the PSNR was above the standard average, although in some images there were many fine vessels that could not be separated from the background. Even so, the value of accuracy obtained is quite high. The purpose of this study is to show that the Otsu Multilevel Thresholding method with levels that have been determined can be effectively considered a good alternative for image segmentation.

ACKNOWLEDGMENT

This article is partly supported by by Direktorat Riset dan Pengabdian Masyarakat, Direktorat Jenderal Penguatan Riset dan Pengembangan, Kementerian Riset, Teknologi dan Pendidikan Tinggi Indonesia and Rector of University of Sriwijaya.

REFERENCES

- [1] Isabel. N. Figueiredo, Susana Moura, Julio S. Naves, Luis Pinto, Sunil Kumar, Carlos M. Oliveira, and João D. Ramos, "Automated retina identification based on multiscale elastic registration," *Computers in Biology and Medicine.*, vol. 79, no. December 2016, pp. 130–143, 2016..
- [2] N. Brancati, M. Frucci, D. Gagnaniello, D. Riccio, V. Di Iorio, and L. Di Perna, "Automatic Segmentation of Pigment Deposits in Retinal Fundus Images of Retinitis Pigmentosa," *Computerized Medical Imaging and Graphics.*, vol. 66, no. June 2017, pp. 73–81, 2018.
- [3] Z. Jiang, H. Zhang, Y. Wang, and S. Ko, "Retinal blood vessel segmentation using fully convolutional network with transfer learning," *Computerized Medical Imaging and Graphics.*, vol. 68, no. July 2017, pp. 1–15, 2018.
- [4] Erwin, Saparudin, M. Fachrurrozi, A. Wijaya, and M. N. Rachmatullah, "New Optimization Technique to Extract Facial Features," *IAENG International Journal of Computer Science.*, vol. 45, no. 4, pp. 523-530, 2018.
- [5] Z. Sufyanu, F. S. Mohamad, Abdulganiyu A. Yusuf, and M. B. Mamat, "Enhanced Face Recognition Using Discrete Cosine Transform," *Engineering Letters.*, vol. 24, no. 1, pp. 52–61, 2016.
- [6] B. Poon, M. Ashrafal Amin, and H. Yan, "PCA Based Human Face Recognition with Improved Methods for Distorted Images due to Illumination and Color Background," *IAENG International Journal of*

- Computer Science.*, vol. 43, no. 3, pp. 277-283, 2016.
- [7] K. Hajari, U. Gawande, and Y. Golhar, "Neural Network Approach to Iris Recognition in Noisy Environment," *Procedia Computer Science.*, vol. 78, no. December 2015, pp. 675-682, 2016.
- [8] A. Maharjan, "Blood Vessel Segmentation from Retinal Images," *Master's thesis, University of Eastern Finland*, no. June, p. 1-88, 2016.
- [9] M. Hassan, M. Amin, I. Murtaza, A. Khan, and A. Chaudhry, "Robust Hidden Markov Model based intelligent blood vessel detection of fundus images," *Computer Methods and Programs in Biomedicine.*, vol. 151, no. November, pp. 193-201, 2017.
- [10] F. Huang, B. Dashtbozorg, T. Tan, and B. M. ter Haar Romeny, "Retinal artery/vein classification using genetic-search feature selection," *Computer Methods and Programs in Biomedicine.*, vol. 161, no. July, pp. 197-207, 2018.
- [11] Erwin, Saparudin, and W. Saputri, "New Hybrid Multilevel Thresholding and Improved Harmony Search Algorithm for Image Segmentation," *International Journal of Electrical and Computer Engineering*, vol. 8, no. 6, pp. 4593-4602, 2018.
- [12] K. Chen, Y. Zhou, Z. Zhang, M. Dai, Y. Chao, and J. Shi, "Multilevel Image Segmentation Based on an Improved Firefly Algorithm," *Mathematical Problems in Engineering.*, vol. 2016, pp. 1-12, 2016.
- [13] Y. Liu, C. Mu, W. Kou, and J. Liu, "Modified particle swarm optimization-based multilevel thresholding for image segmentation Modified particle swarm optimization-based multilevel thresholding for image segmentation," *International Journal of Engineering Technology.*, vol. 19, no. May 2015, pp. 1311-1327, 2016.
- [14] M. H. Mozaffari and W. Lee, "Convergent heterogeneous particle swarm optimization algorithm for multilevel image thresholding segmentation," *The Institution of Engineering and Technology.*, vol. 11, no. 8, pp. 605-619, 2017.
- [15] H. Maryam, A. Mustapha, and J. Younes, "A multilevel thresholding method for image segmentation based on multiobjective particle swarm optimization," *2017 International Conference on Wireless Technologies, Embedded and Intelligent Systems (WITS)*, Fez, Morocco, pp. 1-5, 2017.
- [16] Z. Guo, X. Yue, G. Liu, S. Wang, and K. Li, "An improved harmony search algorithm for multilevel image segmentation," *Innovative Computing, Information and Control Express Letter.*, vol. 9, no. 9, pp. 2531-2536, 2015.
- [17] R. Singh, P. Agarwal, M. Kashyap, and M. Bhattacharya, "Kapur 's And Otsu 's Based Optimal Multilevel Image Thresholding Using Social Spider and Firefly Algorithm," *International Conference on Communication and Signal Processing.*, India, no. April, pp. 2220-2224, 2016.
- [18] A. Hoover, D. Ph, V. Kouznetsova, D. Ph, and M. Goldbaum, "Locating Blood Vessels in Retinal Images by Piece-wise Threshold Probing of a Matched Filter Response Department of Ophthalmology University of California , San Diego," *IEEE Transactions on Medical Imaging*, vol. 19, no. 3, pp. 203-210, 2000.
- [19] A. Das, *Guide to Signals and Patterns in Image Processing*. Springer International Publishing, 2015.
- [20] Erwin, Saparudin, A. Nevriyanto and D. Purnamasari, "Performance Analysis of Comparison between Region Growing , Adaptive Threshold and Watershed Methods for Image Segmentation," *Proceedings of the International MultiConference of Engineers and Computer Scientists*, Hongkong, vol. I, pp. 157-163, 2018.
- [21] Y. Kristian, H. Takahashi, I. K. E. Purnama, K. Yoshimoto, E. I. Setiawan, E. Hanindito, and M. H. Purnomo., "A Novel Approach on Infant Facial Pain Classification using Multi Stage Classifier and Geometrical-Textural Features Combination," *IAENG International Journal of Computer Science.*, vol. 44, no. 1, pp. 112-121, 2017.
- [22] L. Câmara Neto, G. L. B. Ramalho, J. F. S. Rocha Neto, R. M. S. Veras, and F. N. S. Medeiros, "An unsupervised coarse-to-fine algorithm for blood vessel segmentation in fundus images," *Expert Systems with Applications*, vol. 78, no. February, pp. 182-192, 2017.



Erwin was born in Palembang, Indonesia, in 1971. He received his Bachelor of Mathematics from Sriwijaya University, Indonesia, in 1994, and an M.Sc. degree in Actuarial from the Bandung Institute of Technology (ITB), Bandung, Indonesia, in 2002. In 1994, he joined Sriwijaya University, as a Lecturer. Since

December 2006, he has been with the Department of Informatics, Sriwijaya University, where he was an Assistant Professor, becoming an Associate Professor in 2011. Since 2012, he has been with the Department of Computer Engineering, Sriwijaya University. Then, in 2019, he received his Doctorate in Engineering, Faculty of Engineering, Sriwijaya University. His current research interests include image processing, and computer vision. Dr. Erwin, S.Si., M.Si is a member of IAENG and IEEE.



Arfattastury Noorfizir was born in Prabumulih, Indonesia, in 1996. She is currently working on a project for her undergraduate degree at at Computer Engineering Department, Faculty of Computer Science, Sriwijaya University, Indonesia. In 2016, she joined the Laboratory of Image Processing, Sriwijaya University, as Assistant Lecturer. Her current research includes in the field of image processing, pattern recognition and computer vision.



Muhammad Naufal Rachmatullah was born in Surakarta, Indonesia in 1992. He has already been a research assistant at Department of Informatics, University of Sriwijaya Palembang, Indonesia since 2015. He received the Bachelor degree in Informatics from the University of Sriwijaya, Indonesia, in 2015. Currently He is part of a intelligent system research group. His research interests include image processing, computer vision, and machine learning.



Saparudin was born in Pangkal Pinang, Indonesian, in 1969. He received the Bachelor degree in mathematic education from the University of Sriwijaya, Indonesian, in 1993, and the M.Tech. degrees in informatics from the Bandung Institute of Technology (ITB), Bandung, Indonesian, in 2000 and

Ph.D. degrees in computer science from the Malaysian University of Technology (UTM), Johor Bahru, Malaysian, in 2012. In 1995, he joined, University of Sriwijaya, as a Lecturer. Since December 2006, he has been with the Department of Informatics Engineering, University of Sriwijaya, where he was an Assistant Professor, became an Associate Professor in 2011, and a Professor in 2017. His current research interests include image processing, and computer vision. Drs. Saparudin, M.T., Ph.D. is a member of Institute of Advanced Engineering and Science (IAES) and IEEE.



Ghazali Sulong is a Professor in Image processing, Management & Science University, Malaysia. He received the B.Sc. in Statistics from Universiti Kebangsaan Malaysia in 1979, The M.Sc. and Ph.D. degrees in Computing from University of Wales, College of Cardiff, Wales, United Kingdom, in 1982 and 1989, respectively. His current research

interest includes; image processing, computer vision, pattern recognition, and multimedia.